



OPEN

SUBJECT AREAS:
COLLOIDS
LIQUID CRYSTALSReceived
16 October 2014Accepted
13 November 2014Published
5 December 2014Correspondence and
requests for materials
should be addressed to
S.Č. (simon.copar@
fmf.uni-lj.si)

Topological Switching and Orbiting Dynamics of Colloidal Spheres Dressed with Chiral Nematic Solitons

T. Porenta¹, S. Čopar^{1,2,3}, P. J. Ackerman^{4,5}, M. B. Pandey⁴, M. C. M. Varney⁴, I. I. Smalyukh^{4,5,6,7} & S. Žumer^{1,2}

¹Faculty of Mathematics and Physics, University of Ljubljana, Jadranska 19, 1000 Ljubljana, Slovenia, ²J. Stefan Institute, Jamova 39, 1000 Ljubljana, Slovenia, ³Department of Physics and Astronomy, University of Pennsylvania, 209 South 33rd Street, Philadelphia, Pennsylvania 19104, USA, ⁴Department of Physics, University of Colorado, Boulder, CO 80309, USA, ⁵Department of Electrical, Computer, and Energy Engineering, University of Colorado, Boulder, CO 80309, USA, ⁶Liquid Crystal Materials Research Center and Materials Science and Engineering Program, University of Colorado, Boulder, CO 80309, USA, ⁷Renewable and Sustainable Energy Institute, National Renewable Energy Laboratory and University of Colorado, Boulder, CO 80309, USA.

Metastable configurations formed by defects, inclusions, elastic deformations and topological solitons in liquid crystals are a promising choice for building photonic crystals and metamaterials with a potential for new optical applications. Local optical modification of the director or introduction of colloidal inclusions into a moderately chiral nematic liquid crystal confined to a homeotropic cell creates localized multistable chiral solitons. Here we induce solitons that “dress” the dispersed spherical particles treated for tangential degenerate boundary conditions, and perform controlled switching of their state using focused optical beams. Two optically switchable distinct metastable states, toron and hopfion, bound to colloidal spheres into structures with different topological charges are investigated. Their structures are examined using Q-tensor based numerical simulations and compared to the profiles reconstructed from the experiments. A topological explanation of observed multistability is constructed.

Soft matter outperforms solid state materials in reconfigurability, capabilities of self-assembly and self-healing. Strong response to electric fields, optical manipulation and other external stimuli enables efficient control over internal structure of anisotropic and composite soft materials. While soft biological systems already exhibit remarkable complexity and versatility, artificial soft matter is still an emerging, but rapidly evolving field, increasing in complexity of new materials, reliability of microstructural assembly, and readiness for technological applications. Liquid crystals and their composites are, due to their optical anisotropy and simplicity of electrical and optical manipulation^{1–3}, a common choice for creating micro devices⁴, photonic and lasing elements^{5–8} and micro sensors^{9–13}. Configurations with multiple stable states that can be reliably switched are a basis for commercial-grade display devices, optical switches and phenomena involving memory effects^{14,15}. Topological defects, solitons and knotting coupled with particle inclusions are lately being researched as means for achieving switchable metastable states and self-assembly^{16–18}.

In nematic liquid crystals, molecules align along a local preferred direction called the director. The director, a vector-like quantity without distinction between diametrically opposite directions (headless vector), forms point-like and line-like topologically stable defects, especially when boundary conditions disallow a defect-free state^{19–23}. In a cholesteric liquid crystal, the director field prefers to helically twist along a certain direction called the helical axis. In a cell with homeotropic anchoring at its boundaries, the helical structure is hindered by boundary conditions that prefer a homogeneous director field. When the cholesteric pitch is comparable to the cell thickness, we obtain a frustrated environment where localized chiral excitations can be created and erased by manipulation with focused laser beams²⁴ and an external electric field²⁵. This led to the discovery of solitons such as torons²⁶ and hopfions (Hopf fibrations in director field)²⁷ which, once created, behave as quasi-particles that are stable to small perturbations. In achiral and moderately twisted nematics, particles with various surface treatments are “dressed” by a relatively thin layer of elastic distortions with topologically required boojums and point and line defects. Unlike the more commonly occurring point and line defects, standalone torons and hopfions in frustrated cholesterics occur on a much larger length scale, set by the cholesteric pitch. They are topologically stable on their own due to entanglement of the entire nematic texture, not just the cross section in



the vicinity of the singular regions. While stable isolated solitons are interesting both from a theoretical as well as applied scientific standpoint, inclusion of particles fuses the topological versatility of solitons with the structural potential of colloidal lattices. This opens a great variety of particle-soliton bound states to explore.

In this work, we present the structure and manipulation of topological solitons coupled with colloidal microspheres in a homeotropic chiral nematic cell – a thin slab of cholesteric confined between parallel surface-treated glass plates. In a range of thickness over equilibrium cholesteric pitch values ~ 0.8 to 0.95 and microsphere diameter ~ 0.7 of the thickness, we identify solitonic nematic field configurations that are stabilized by the medium's chirality and form hybrid structures with the microspheres. With polarizing optical microscopy (POM) textures, we demonstrate optical switching between multiple stable or metastable (stable under small perturbations) hybrid structures and their manipulation. Using optical manipulation of the LC director field and three dimensional (3D) imaging techniques, we gain insight into the confined hybrid system's surface and bulk topology. Predictably, the 2D topology of the microsphere surface field is bound to the 3D field topology of the surrounding soliton. Multistable twisted solitons that arise due to the interplay of confinement and chirality can be optically and magnetically controlled and manipulated.

Results

In Figure 1 we show co-existence of several structural states in a confined chiral nematic, comprised of different combinations of spherical particles, torons, hopfions, and bulk and surface point defects. The prominent swirls seen in POM textures arise due to broken symmetry about the cell mid-plane²⁸. This hybrid structure is identical for opposite swirls but flipped top for bottom (Fig. 1c). Hopfion dressed microspheres with “swirls” in Fig. 1c indicate that the microsphere is above or below the mid-plane of the cell and the amount of twisted LC above and below the microsphere is unequal. The toron-dressed microsphere is always observed with swirls due to its inherent asymmetry; however, the hopfion dressed microsphere can be either asymmetric (Fig. 1a–c) or symmetric (Fig. 1d) with respect to cell mid-plane. A hopfion-dressed microsphere without “swirls” occurs when the microsphere is centered in the cell mid-plane. This experimentally less common hybrid structure forms in a thicker region of the cell $\sim 11 \mu\text{m}$. When particle size is reduced even further relative to the cell thickness and cholesteric pitch p ($p/2$ or smaller), one often also observes microspheres localizing on the

central axis of the double twist torus (Fig. 1e). Using superparamagnetic particles rotated by rotating magnetic fields, we observed that the studied solitonic structures are all stable with respect to particle rotation, although this rotation in the case of the structure shown in Fig. 1e results in its orbital motion inside the double twist torus (Figs. 5 and 6).

In addition to POM images, we study the director around hopfion and toron dressed microparticles through the use of three-photon excitation fluorescence polarizing microscopy (3PEF-PM), which retrieves the angle of the local director relative to the light polarization (Fig. 2). Combining data at different polarizations allows one to reconstruct the details of complex three-dimensional director fields²⁷. We also use a circularly polarized excitation beam to further distinguish the structures according to where the director aligns predominantly parallel to the confining substrates (see Fig. 2b, d). Both the bright field images and the 3PEF-PM cross section resemble the looped double-twist tubes seen in free-standing torons and hopfions^{26,27}, which exist due to locally introduced twist that serves to relieve frustration of a cholesteric caused by homeotropic surface boundary conditions.

To confirm the validity of our proposed director model, both states were reproduced with Landau-de Gennes numerical simulation (Fig. 2e, g and Fig. 3). We constructed a chiral nematic cell of dimensions $6 \mu\text{m} \times 6 \mu\text{m} \times 3 \mu\text{m}$ filled with a chiral material with an equilibrium pitch of 0.85 times the cell thickness and a spherical particle with diameter equal half of the cell thickness (the method is further discussed in the supplementary material). Initial condition was constructed to match the experimental data, albeit scaled down to avoid computational limitations. As the equilibrium state is scale-invariant in the director representation of the nematic, the rescaling affects the stability of defects, but gives a good approximation to the director state in the bulk. A double-twist cylinder, a structure well known from the study of blue phases²⁹, was imposed into a toroidal configuration in order to construct initial condition for toron structures²⁶. A relaxation method was used to find free energy minima at a given particle position^{30,31}. The vertical position of the particle was adjusted to reach the true free energy minimum of its equilibrium state. Numerical and experimental results for both metastable structures were visualized by using isosurfaces of the magnitude of director projection along two orthogonal horizontal directions (Fig. 2e–h)³². Even considering finite resolution and noise in the experimental data, the 3PEF-PM structures show a qualitative agreement, confirming our reconstruction of the director.

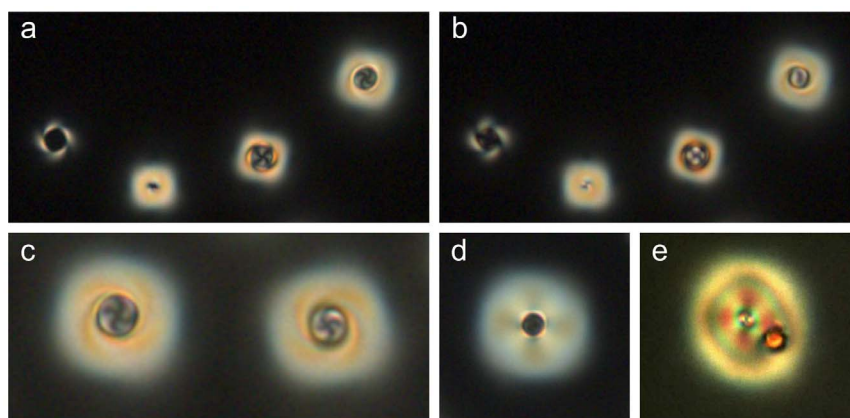


Figure 1 | POM micrographs of microsphere-soliton hybrids in frustrated cholesteric LCs. (a), (b), POM micrographs obtained for two different levels of the microscope's focal plane (a), above and (b), below the cell midplane. The structures are (from left to right): (1) A bare colloidal microsphere with two boojums surrounded by minor distortions, (2) a triple twist toron with two bulk point defects, (3) a toron dressed microsphere with one bulk point defect, (4) and a hopfion dressed microsphere. (c), Two hopfion dressed microspheres at different levels of the sample. (d), A hopfion dressed microsphere located in the midplane of the sample. (e), a toron in a 5CB-based CLC that is smaller colloidal sphere with its center located on the central axis of the looped double-twist cylinder. The diameters of colloidal particles are $7 \mu\text{m}$ in (a–d) and $4.5 \mu\text{m}$ in (e).

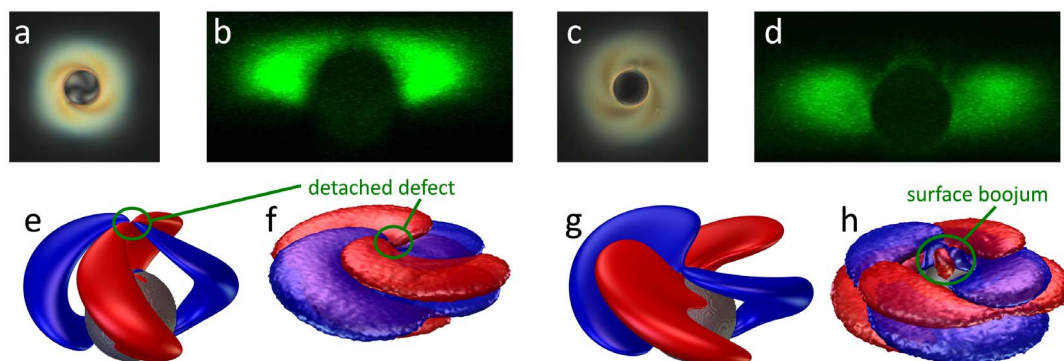


Figure 2 | Metastable twisted textures around colloidal particles with degenerate planar surface anchoring. (a), (b), (e), (f): A structure, recognized as a toron, bound to a colloidal particle. (c), (d), (g), (h): A hopfion, bound to a colloidal particle. Viewed between crossed polarizers (a), (c), the structures swirl in opposite directions due to different vertical particle positions. Cross sections with circularly polarized 3PEF-PM (b), (d) reveal existence of a bulk point defect only for the toron structure. (e), (f), (g), (h) show the regions of maximum intensity of linearly polarized 3PEF-PM signal for two perpendicular polarizations, extracted from numerical modeling and experimental imaging. Notice that the toron structure has a detached defect (e), (f), while the hopfion has just a surface boojum (g), (h). The diameter of particles is 7 μm .

A particle with planar degenerate anchoring by itself requires existence of surface defects, which manifest as boojums at the poles of the particle²¹. Both observed structures retain cylindrical symmetry with two boojums at the poles, but break the chiral symmetry

by having the director turn in-plane on the particle surface instead of pointing along the meridians. The structure in Fig. 3a has one small ring defect in bulk and resembles the toron structure with one of the defects replaced by a spherical particle. Following the surface from

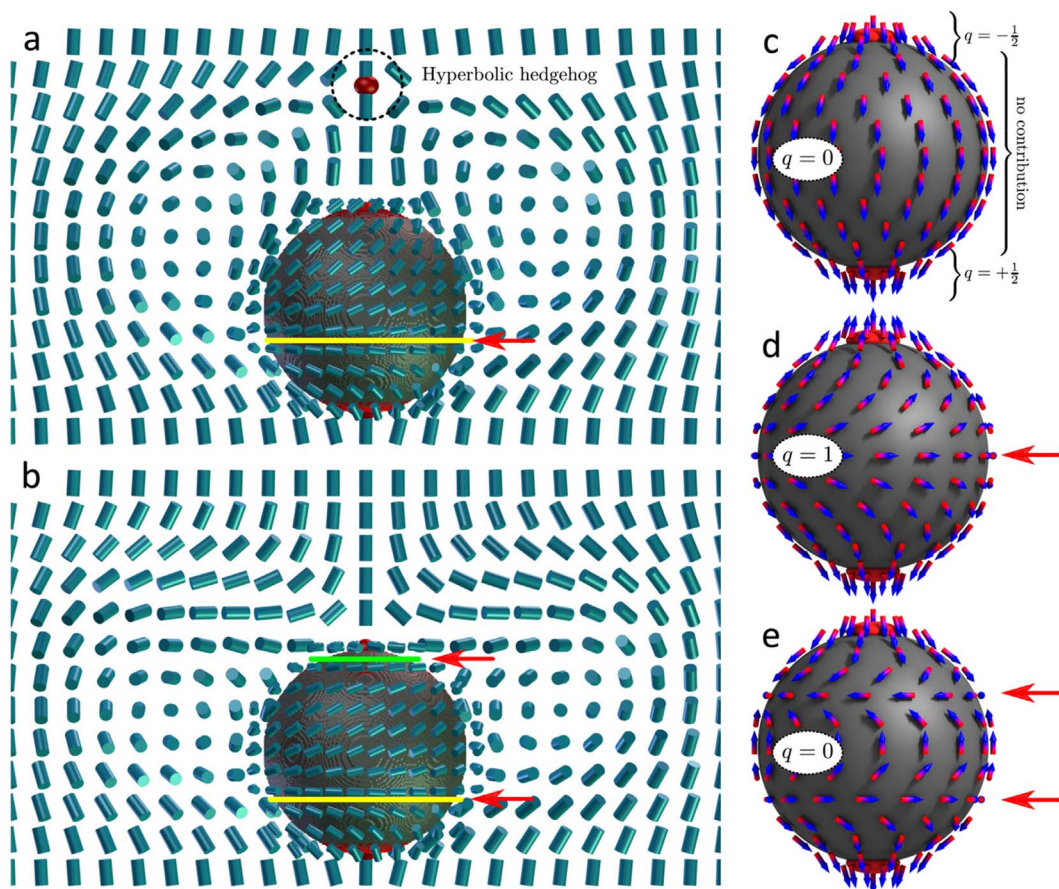


Figure 3 | Topological analysis of director field textures. (a), (b) Numerically obtained structures in vertical cross section with director marked with cylinders and defects shown as red isosurfaces. Similarly to experiments, both structures are found to be (meta)stable: (a) Toron-dressed particle with one point defect in bulk and one turn of the director on particle surface (indicated by an arrow) and (b) Hopfion-dressed structure without bulk defects with two opposite director turns on the particle surface. In-plane turns are found by marking the horizontal (quarter-turn) director with yellow (clockwise) or green (counterclockwise) line. (c–e) A theoretical model reveals that only the boojums contribute to the topological charge q of the whole, so the charge only depends on the arrow directions at the boojums (the director's arrow, marked also with colored tips, holds no physical significance for the nematic). Compare (a) to (d). The latitudes with horizontal director field are indicated by arrows. Note that (b) consists of two opposite turns and thus corresponds to the structure (c) instead of (e), although both have the same topological charge. The intrinsic pitch in simulations (a), (b) is 0.85 of the cell thickness.



the bottom to the top pole, the director makes a π -turn in-plane. In contrast, the structure in Fig. 3b does not have any bulk defects and resembles the hopfion structure²⁷. The director only swivels on the particle surface, amounting to a zero total turning angle, and is thus distorted, but topologically equivalent to the structure expected in achiral nematics (Fig. 3c).

The difference in the number of point defects in the bulk suggests the particle with its boojums carries a different charge in either structure, which deserves a quick digression into the topology of the textures. By the Poincaré theorem^{33,34}, director field on a sphere with degenerate planar anchoring cannot exist without surface boojums with total winding number of 2, which is in our experiments and simulations fulfilled by a pair of boojums with winding number of +1 at the poles. The colloidal particle together with both boojums can be assigned a topological charge assuming that the director is consistently decorated with arrows to obtain a true vector field. Following a similar procedure to the topological analysis of spherical droplets in Ref. 33, we cut the surface into two infinitesimally small circular patches around the boojums, each contributing $\pm 1/2$ to the expression for the topological charge, and the rest of the surface with a vanishing contribution. Note that while evaluation of the topological charge benefits from this splitting, only the final integer result is topologically relevant. The sign of the boojum's contribution is positive if the director points outwards at the tip of the boojum and vice-versa. The degree of freedom that determines the relative sign of the boojums is the in-plane rotation of the director with changing polar angle (latitude), which can amount to any integer number of π -turns. Zero turns corresponds to the particle with a planar degenerate anchoring in an achiral nematic, which is known to have a zero topological charge, $q = 0$ (Fig. 3c). With an increasing number of turns, the topological charge of these hypothetical structures alternates between $q = \pm 1$ and $q = 0$ (Fig. 3d, e). The number of turns is easily determined by counting the latitudes where the director points in a horizontal (east-west) direction, taking into account the sense of

director rotation. In the hopfion structure, the director is turning back and forth to accommodate the soliton around the particle, but amounts to an even number of turns (zero, in particular) and thus has zero topological charge with no additional defects required (Fig. 3b). The toron structure (Fig. 3a) has one turn and therefore topological charge $q = \pm 1$, which explains the additional hyperbolic hedgehog in the bulk.

Unlike an achiral nematic, where distortions tend to be localized around the particle, the deformation of the director field extends more than a diameter away from the particle. From our experiment, we can conclude that the presence of a particle with degenerate planar anchoring binds and stabilizes the position of the soliton, but does not alter the integrity of its texture or its optical signature. We demonstrate optical switching and manipulation of microsphere-soliton hybrids. Focusing a laser beam in the cell mid-plane nearby a particle with different polarizations allows for inducing transformations of the bare microsphere with boojums into a hopfion-dressed state (Fig. 4a–d and the supplementary movie S1), and vice-versa (Fig. 4e–h and supplementary movie S2). Although boojums attached to microspheres could not be optically manipulated as individual objects (supplementary movie S4), the bulk point defect of the toron-dressed microsphere could be manipulated individually (Fig. 4i–l and supplementary movies S3). Switching between both structures with optical tweezers corresponds to switching between torons and hopfions²⁷, but with more control and reliability enabled by the local-twist-stabilizing effect of colloids.

When a colloidal particle is smaller than half the size of a toron, we find experimentally that the location of this particle within the double twist cylinder is in at least a metastable state, and often a ground state. Figure 5 shows a case where the spherical colloidal particle is a superparamagnetic bead (SPMB) with tangential surface anchoring embedded in a toron such that its center of mass roughly seats on the central line of a looped double twist cylinder. The director at the surface of the particle is in the bipolar state with two boojums at

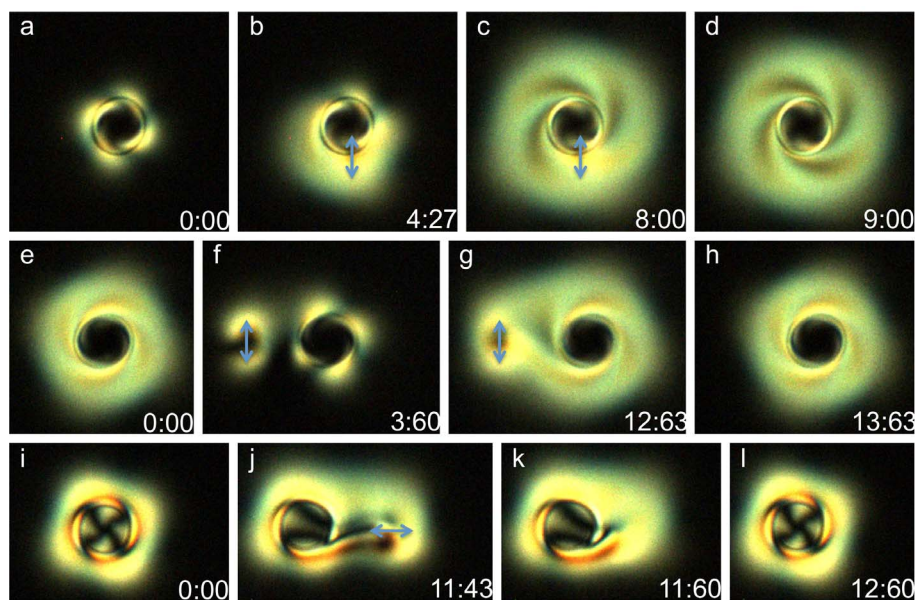


Figure 4 | Optical switching and manipulation of microsphere-soliton hybrids. POM images with a blue double-sided arrow approximately indicating where and when the laser was turned on or off and laser polarization orientation. Lower right numbers indicate the elapsed time corresponding to the supporting information movies. (a–d), a laser induced hopfion surrounding a microsphere. (a), the bare microsphere surrounded by minor elastic distortions. (b), moments after the laser was introduced to the sample. (c), the hopfion structure fully formed and (d), after the laser is removed and the structure is fully relaxed. (e–h), optical switching of a hopfion-dressed microsphere. (e), the initial hopfion dressed microsphere switched to (f), a bare microsphere with a laser induced distortion that has opposing twist. (g), the hopfion induced again with the same laser position but with opposite twist. (h), the final configuration after laser is removed. (i–l), a toron-dressed microsphere's bulk point defect manipulated with a laser. (i), the initial toron dressed microsphere. (j), after pulling the hyperbolic hedgehog of the toron structure away from the microsphere. After removing the laser (k), the bulk defect begins to return to the microsphere. (l), the final relaxed configuration. The diameter of particles is 7 μm .

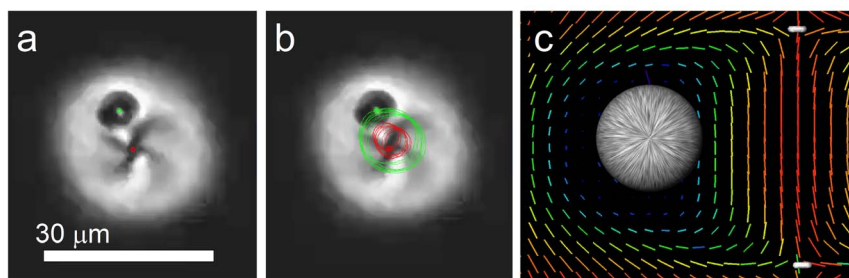


Figure 5 | A SPMB microsphere within a toron's double twist cylinder. (a), A SPMB (center of mass highlighted with a green dot) embedded within the double twist cylinder of a toron (denoted by a red dot.) (b), Motional tracks of the SPMB and toron center of mass (green and red respectively) shows an orbital path around a particle/toron barycenter. (c), Simulated director field around a SPMB located at the axis of the double twist cylinder. The diameter of the $4.5 \mu\text{m}$ SPMB is roughly a quarter of the cell thickness. The director on the particle's surface is dipolar with two boojums, as visualized by the streaks. The red-to-blue color gradient encodes the out-of-plane component of the director, the blue marking the core of the double-twist cylinder.

the poles of the particle (Fig. 5c). The boojums orient in the direction of the central loop of the double twist cylinder, which a small enough particle feels as an approximately homogeneous field tangential to the centerline of the torus. Due to the viscous coupling of the particle with the surrounding medium, rotation of the particle induces rotation of the boojums and consequently, motion of the particle within the double twist cylinder.

The SPMB was first optically co-located within the double twist cylinder of a toron, which can be a stable or metastable position of such a particle with respect to a toron or hopfion, depending on the relative size of the particle with respect to the size of the toron. A 105 Gs magnetic field rotating at 0.125 Hz was applied in the x - y plane to rotate the SPMB³⁶, which when coupled via surface interactions with the local director induces a so-called “orbital” motion

(Fig. 6). This orbital motion is in the same sense as the rotating magnetic field and can be reversed by reversing the latter. Importantly, unlike optical manipulation that allows one to switch between different topological configurations, magnetic manipulation only affects the SPMB and leaves the topology of solitons intact, since these structures are robust with respect to perturbations caused by the presence and motion of small particles within the double-twist region. Figure 6a shows this orbital motion with respect to the toron center reference frame. SPMB radius and angle vary with time (black and green lines respectively) as referenced to the toron center of mass. The red line represents the angle of the magnetic field which rotates at $\pm 45 \text{ deg/s}$. Interestingly, average orbital radius is $5.1 \mu\text{m}$ for a clockwise orbit, and $5.6 \mu\text{m}$ for a counterclockwise orbit, which is natural as the soliton structure is chiral. The magenta dotted line

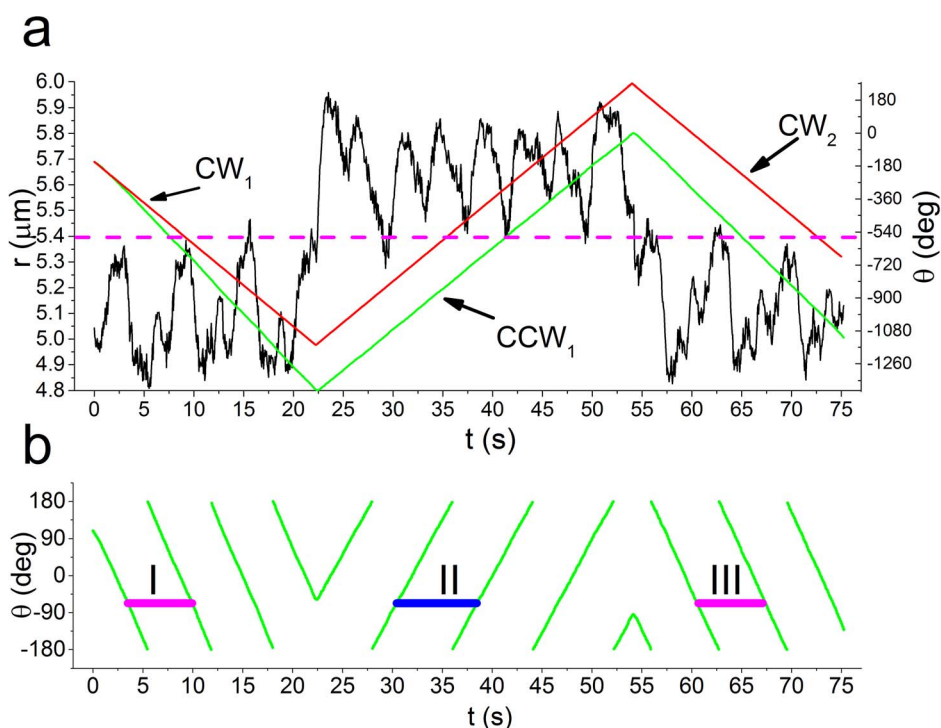


Figure 6 | SPMB motion within a toron induced by a rotating magnetic field. (a) Motional analysis of the SPMB “orbiting” the toron center reference frame. SPMB radius and angle vs. time (black and green lines respectively) as referenced to the toron center. The red line depicts the angle of the magnetic field with respect to Cartesian reference frame as it is rotated at 45 deg/s . Average orbital radius is $5.1 \mu\text{m}$ for clockwise (CW) orbit, and $5.6 \mu\text{m}$ for a counterclockwise (CCW) orbit. The magenta dotted line represents the equilibrium position of the SPMB when not being magnetically manipulated. Periodic oscillations of this orbital radius are evident. The average angular velocity for CW_1 is -57 deg/s , for CW_2 45 deg/s , and for CW_3 is -53 deg/s . (b) Orbital polar angle vs. time indicating asymmetry in orbital angular velocity and period depending on the field rotation direction. Note period and slope differences between regions I, II and III and symmetry between regions I and III.



represents the equilibrium position of the SPMB when it is not being acted on by the rotating magnetic field. Periodic oscillations of the orbital radius during rotation are evident. The average angular velocity for the region CW_1 marked on the figure is -57 deg/s, for CW_2 is 45 deg/s, and for CW_3 is -53 deg/s. The dependence of the orbital angle vs. time indicates asymmetry in orbital angular velocity and shows that the period depends on the field rotation direction.

Discussion

Our particle-stabilized solitons add to the set of manipulable objects in frustrated cholesteric liquid crystals. Controlled creation and annihilation of an extra point defect is a bistable process; a desirable property in display and memory devices. The chirality of the medium thus unlocks the ability to exert active control over the topological charge of the particle, if the particle size is comparable to the pitch. Smaller particles are attracted to defects and places with high elastic deformation and in the chiral solitons structure, become confined by the double-twist torus. These solitons can thus act as “invisible” channels without the need for solid confining surfaces. Allowing multiple particles and quasi-particles to interact in the medium opens new possibilities for self-assembly and targeted assembly of super-structures with optical applications. The particles contribute their tendency to form lattices and act as a way of pinning the solitons, which contrasts to standalone solitons, which behave as unbound particles and are free to move around the sample. Coexistence of both microsphere-bound and free quasi-particles suggests composite materials and devices based on transport of the solitons in a custom-built environment, possibly driven by flow. If the particle size, surface anchoring, and cholesteric pitch are varied, the properties can be fine-tuned to fit the design in mind.

Manipulation of particles of various sizes is a versatile way of creating new structures and exploiting phenomena for their optical response, rheology or combination of responses to different fields and stimuli. In a frustrated chiral environment, we demonstrate that the set of switchable structures with strong optical response is enriched even more with coupling to twisted chiral nematic solitons, leading to dressing of larger particles and confinement and guidance of smaller particles. The research of soliton-particle interaction is a stepping stone toward superstructures with topologically ensured stability and flexible design, illuminating the path toward future development.

Methods

A chiral nematic liquid crystal (CNLC) host is prepared by introducing chiral additive S-811 (EM Chemicals) to a commercial nematic LC AMLC-0010 (Alphamicon, Inc.). Alternatively, we also used samples made from pentylcyanobiphenyl (5CB, from Frinton Laboratories) doped with chiral dopant cholesteryl nonanoate (Sigma-Aldrich). The value of the pitch $p = 1/(h_{HTP} \times C_{chiral})$ of CNLC of interest is set by choosing an appropriate concentration C_{chiral} of the chiral dopant in the nematic host for the known value of the so-called “helical twisting power” h_{HTP} ^{25,26}. We use Melamine resin particles of diameter ~ 7 μm and superparamagnetic beads (SPMBs) of diameter ~ 4.5 μm (DynaBead M450, Invitrogen) fabricated from ~ 8 nm ferromagnetic nanoparticles ($\gamma\text{-Fe}_2\text{O}_3$ and Fe_3O_4) embedded into a highly cross-linked epoxy matrix. Both types of particles have tangential surface anchoring. The mixture of CNLCs and microparticles was sonicated for 10 h to obtain a uniform distribution. LC cells are enclosed between glass plates. Strong vertical surface alignment on the inner surfaces of the confining glass plates is set by treating these substrates with N,N-dimethyl-n-octadecyl-3-aminopropyltrimethoxysilyl chloride (DMOAP) by means of dip-coating in a 1 wt% aqueous solution^{26,27}. LC cells with the cell gap thickness $d = 5\text{--}30$ μm are produced by sandwiching glass substrates interspaced by glass fiber segments of corresponding diameter. CNLCs colloidal dispersions are then infused into the cell of thickness less than the pitch of CNLCs by capillary forces at room temperature. We seal the cells with epoxy.

Optical manipulation and 3D imaging was performed with an experimental setup composed of holographic optical tweezers (HOT) and three-photon excitation fluorescence polarizing microscopy (3PEF-PM) built around an inverted microscope IX 81 (Olympus). HOT utilizes a reflective, phase-only spatial light modulator (SLM) (Boulder Nonlinear Systems) and an Ytterbium-doped fiber laser (YLR-10-1064, IPG Photonics) operating at 1064 nm. The SLM controlled the phase of the laser beam on a pixel-by-pixel basis according to the computer-generated holographic patterns at a refresh rate of 30 Hz. This phase-modulated beam was imaged at the back aperture of the microscope objective while creating the spatial trap intensity pattern in a sample.

For 3PEF-PM imaging, we have employed a tunable (680–1080 nm) Ti-Sapphire oscillator (Chameleon Ultra II, Coherent) emitting 140 fs pulses at a repetition rate of 80 MHz. The laser wavelength was tuned to 870 nm for the three-photon excitation of 5CB molecules. The 3PEF-PM signal was collected in epi-detection mode with a photomultiplier tube (H5784-20, Hamamatsu). An Olympus 100 oil-immersion objective with high numerical aperture of 1.4 was used for both imaging and optical trapping. A detailed description of these experimental setups is found in refs. 2,35.

Rotational manipulation of magnetically responsive particles was achieved using an in-house, custom-built magnetic manipulation system integrated within the same optical imaging and manipulation setup³⁶. This provided a robust method for magnetic and optical non-contact manipulation in a fully holonomic manner, i.e., in all three Cartesian degrees of freedom via holographic optical tweezers (used to co-locate particles with torons or hopfions, but then turned off) and in all three rotational degrees of freedom via magnetic control. Magnetic field rotation is achieved using three iron-core electromagnets arranged in a Cartesian frame machined from aluminum and mounted directly on the microscope body, with each electromagnet independently driven via an amplified power supply controlled using a computer-controlled data acquisition and in-house software³⁶.

Computer simulations of the CNLC medium use the extended Landau-de Gennes free energy model³⁶. In the one elastic constant approximation, distortion free energy is expanded in powers of the order parameter tensor and its first derivatives (See Refs. 30, 31, 37). As a model for the experiment, degenerate planar anchoring on particle surface is ensured through construction similar to Fournier and Galatola³⁸. The material constants are taken from³¹, and strong degenerate planar anchoring of $W^d = 10^{-3}$ Jm^{-2} is used to model the surfaces. Boundaries of homeotropic cell are fixed to approximate homogeneous far-field director. Pitch is equal to cell thickness. Mesh resolution is 10 nm.

- Durbin, S. D., Arakelian, S. M. & Shen, Y. R. Optical-field – induced birefringence and Freedericksz transition in a nematic liquid crystal. *Phys. Rev. Lett.* **47**, 1411 (1981).
- Grier, D. G. A revolution in optical manipulation. *Nature* **424**, 810 (2003).
- Trivedi, R. T., Lee, T., Bertness, K. A. & Smalyukh, I. I. Three dimensional optical manipulation and structural imaging of soft materials by use of laser tweezers and multimodal nonlinear microscopy. *Optics Express* **18**, 27658 (2010).
- Santamato, E., Sasso, A., Bruzzese, R. & Shen, Y. R. Intrinsic optical transistor action in homeotropically aligned nematic crystal films. *Optics Letters* **11**, 452 (1986).
- Kang, D., MacLennan, J. E., Clark, N. A., Zakhidov, A. A. & Baughman, R. H. Electro-optic behavior of liquid-crystal-filled silica opal photonic crystals: effect of liquid crystal alignment. *Phys. Rev. Lett.* **86**, 4052 (2001).
- Zografopoulos, D. C., Asquini, R., Kriezis, E. E., d’Alessandro, A. & Beccherelli, R. Guided-wave liquid-crystal photonics. *Lab Chip* **12**, 3598–3610 (2012).
- Humar, M., Ravnik, M., Pajk, S. & Muševič, I. Electrically tunable liquid crystal optical microresonators. *Nat. Photonics* **3**, 595 (2009).
- Humar, M. & Muševič, I. 3D microlasers from self-assembled cholesteric liquid-crystal microdroplets. *Opt. Express* **18**, 26995 (2010).
- Brake, J. M., Daschner, M. K., Luk, Y.-Y. & Abbott, N. L. Biomolecular interactions at phospholipid-decorated surfaces of liquid crystals. *Science* **302**, 2094 (2003).
- Lin, I.-H. *et al.* Endotoxin-induced structural transformations in liquid crystalline droplets. *Science* **332**, 1297 (2011).
- Aliño, V. J., Sim, P. H., Choy, W. T., Fraser, A. & Yang, K.-L. Detecting proteins in microfluidic channels decorated with liquid crystal sensing dots. *Langmuir* **28**, 17571 (2012).
- Scherschener, E. *et al.* Polymer-dispersed liquid-crystal voltage sensor. *Appl. Opt.* **45**, 3482 (2006).
- Humar, M. & Muševič, I. Surfactant sensing based on whispering-gallery-mode in lasing liquid-crystal microdroplets. *Opt. Express* **19**, 19836 (2011).
- Serra, F., Buscaglia, M. & Bellini, T. The emergence of memory in liquid crystals. *Materials Today* **14**, 488 (2011).
- Semenova, Y., Dovgalets, S., Panarin, Y. & Farrell, G. Liquid Crystal Based Optical Switches. *Mol. Cryst. Liq. Cryst.* **413**, 385–398 (2004).
- Tkalec, U. & Muševič, I. Topology of nematic liquid crystal colloids confined to two dimensions. *Soft Matter* **9**, 8140–8150 (2013).
- Senyuk, B. *et al.* Topological colloids. *Nature* **493**, 200–205 (2013).
- Seč, D., Čopar, S. & Žumer, S. Topological zoo of free-standing knots in confined chiral nematic fluids. *Nature Commun.* **5**, 3057 (2014).
- Poulin, P., Stark, H., Lubensky, T. C. & Weitz, D. A. Novel colloidal interactions in anisotropic fluids. *Science* **275**, 1770 (1997).
- Kurik, M. V. & Lavrentovich, O. D. Defects in liquid crystals: homotopy theory and experimental studies. *Sov. Phys. Usp.* **31**, 196 (1988).
- Mermin, N. D. The topological theory of defects in ordered media. *Rev. Mod. Phys.* **51**, 591 (1979).
- Kléman, M. & Lavrentovich, O. D. *Soft Matter Physics: An Introduction*. Springer New York, 2003.
- Kléman, M. *Points, lines and walls: In Liquid Crystals, Magnetic Systems and Various Ordered Media*, Wiley-Interscience Publication, Chichester (1982).
- Porenta, T., Ravnik, M. & Žumer, S. Complex field-stabilised nematic defect structures in Laguerre-Gaussian optical tweezers. *Soft Matter* **8**, 1865 (2012).
- de Gennes, P. G. & Prost, J. *The Physics of Liquid Crystals*. Oxford University Press, Oxford, 1993).



26. Smalyukh, I. I., Lansac, Y., Clark, N. A. & Trivedi, R. P. Three-dimensional structure and multistable optical switching of triple twist toron quasiparticles in anisotropic fluids. *Nat. Mater.* **9**, 139 (2010).
27. Chen, B. G.-g., Ackerman, P. J., Alexander, G. P., Kamien, R. D. & Smalyukh, I. I. Generating the Hopf fibration experimentally in nematic liquid crystals. *Phys. Rev. Lett.* **110**, 237801 (2013).
28. Pandey, M. B. *et al.* Self-assembly of skyrmion-ressed chiral nematic colloids with tangential anchoring. *Phys. Rev. E* **89**, 060502 (2014).
29. Wright, D. C. & Mermin, N. D. Crystalline liquids: the blue phases. *Rev. Mod. Phys.* **61**, 385 (1989).
30. Ravnik, M. *et al.* Entangled nematic colloidal dimers and wires. *Phys. Rev. Lett.* **99**, 247801 (2007).
31. Ravnik, M. & Žumer, S. Nematic colloids entangled by topological defects. *Soft Matter* **5**, 269274 (2009).
32. Copar, S., Porenta, T. & Žumer, S. Visualization methods for complex nematic fields. *Liq. Cryst.* **40**, 1759 (2013).
33. Lavrentovich, O. D. Topological defects in dispersed liquid crystals, or words and worlds around liquid crystal droplets. *Liq. Cryst.* **24**, 117 (1998).
34. Volovik, G. E. & Lavrentovich, O. D. Topological dynamics of defects: boojums in nematic drops. *Sov. Phys. JETP* **58**, 1159 (1984).
35. Lee, T., Trivedi, R. P. & Smalyukh, I. I. Multimodal nonlinear optical polarizing microscopy of long-range molecular order in liquid crystals. *Opt. Lett.* **35**, 3447–3449 (2010).
36. Varney, M. C. M., Jenness, N. J. & Smalyukh, I. I. Geometrically unrestricted topologically constrained control of liquid crystal defects using simultaneous holonomic magnetic and holographic optical manipulation. *Phys. Rev. E* **89**, 022505 (2014).
37. Chandrasekhar, S. *Liquid Crystals*, Cambridge University Press, Cambridge, (1992).
38. Fournier, J.-B. & Galatola, P. Modeling planar degenerate wetting and anchoring in nematic liquid crystals. *EPL* **72**, 403 (2005).

Acknowledgments

We thank T. Lee, B. Senyuk, and J. van de Lagemaat for discussions. This research was supported by the U.S. Department of Energy, Office of Basic Energy Sciences, under Award ER46921 (P.J.A., M.C., M.C.V., M.P., I.I.S.). T.P., S.Č. and S.Ž. acknowledge support from the Slovenian Research Agency under contracts P1-0099. (T.P., S.Č. and S.Ž.) and Z1-6725 (S.Č.).

Author contributions

P.J.A., M.B.P., M.C.V. and I.I.S. devised and performed the experiments. T.P. performed the numerical simulations. S.Č. constructed a topological model and analyzed the data. I.I.S. and S.Ž. supervised the research. All authors contributed to the manuscript.

Additional information

Supplementary information accompanies this paper at <http://www.nature.com/scientificreports>

Competing financial interests: The authors declare no competing financial interests.

How to cite this article: Porenta, T. *et al.* Topological Switching and Orbiting Dynamics of Colloidal Spheres Dressed with Chiral Nematic Solitons. *Sci. Rep.* **4**, 7337; DOI:10.1038/srep07337 (2014).



This work is licensed under a Creative Commons Attribution-NonCommercial-ShareAlike 4.0 International License. The images or other third party material in this article are included in the article's Creative Commons license, unless indicated otherwise in the credit line; if the material is not included under the Creative Commons license, users will need to obtain permission from the license holder in order to reproduce the material. To view a copy of this license, visit <http://creativecommons.org/licenses/by-nc-sa/4.0/>